Performance Benchmark of Yaw Rate Controllers by Active Front Steering

Comparative Analysis of Model Predictive Control, Linear Quadratic Integral Control and Yaw Moment Observer

Kota Miyahara, Hiroshi Fujimoto, Yoichi Hori
Graduate School of Frontier Sciences
The University of Tokyo
Kashiwa, Chiba, Japan
miyahara.kota17@ae.k.u-tokyo.ac.jp

Valentin Ivanov
Automotive Engineering Group
Technische Universität Ilmenau
Ehrenbergstr, Ilmenau, Germany
valentin.ivanov@tu-ilmenau.de

***Abstract*—Although extensive research has been conducted to design active steering controllers for self-driving vehicles, the cross comparison between those controllers has not been studied much yet. Thus, we developed a benchmark to compare yaw rate control methods by active front steering. Three yaw rate controllers, model predictive control, linear quadratic integral control and yaw moment observer-based control, were compared in terms of four evaluation indices: slew rate of actuator input, emergency performance, robustness against disturbance and stability performance of sideslip angle. The comparison was carried out in simulation environment with a 10 DoF vehicle dynamics model validated by an experiment.**

***Index Terms*—active front steering, vehicle motion control, yaw rate control, model predictive control, linear quadratic integral control, yaw moment observer, benchmarking**

I. Introduction

The trend of research and development of self-driving cars are rapid and remarkable recently. Because people have high expectations that the era of self-driving cars will come,the news of the fatal self-driving car's crash [1] gave all the more shock to the world.

Safety is a necessary requirement for practical realization of self-driving cars, and vehicle motion control is one of the mandatory technologes for it [2]. For vehicle motion control, lateral dynamics and yaw stability are significant which are affected by vehicle structure, constants such as mass and wheel tread, vehicle velocity, wheel speed, conditions of the road, and steering angle.

A device called electric power steering (EPS) is used to control the steering angle autonomously. The EPS system uses an electric motor to provide steering torque. The rotational torque is translated into linear force to apply to wheels through a rack-and-pinion. Steering by an actuator is called active steering, especially active front steering (AFS) for front wheels. AFS is effective in the situations in which a vehicle needs to control its yaw motion (e.g., lane change and emergency collision avoidance) and the situations in which the vehicle needs to stabilize its yaw motion (e.g., the case that wheel slip ratios differ between left and right road).

A lot of unique methods have been proposed for vehicle motion control by AFS. The method proposed by Zainal et al., for example, uses PID control for the system with an input of steering angle and outputs of yaw rate and sideslip angle to eliminate the steady state error within 5 seconds [3]. Kim et al. proposed a vehicle position control method by AFS while minimizing a cost fuction defined by position error and control input in the framework of model predictive control (MPC) [4]. Tavan et al. proposed a linear quadratic regulator (LQR) controller for integrated longitudinal and lateral dynamics to follow desired path [5]. Ma et al. used multi-objective sliding mode control considering yaw rate and sideslip angle [6]. By utilizing the charatristics of in-wheel motors which are able to generate yaw moment by the difference of drive torques, Nam et al. proposed 2 degree-of-freedom control with yaw moment observer (YMO) [7].

Although various methods for vehicle motion control related to AFS have been proposed, those methods are based on different preconditions such as control objectives and not compared to each other. Robustness analysis of those control strategies from various perspectives has to be carried out [8].

This paper focuses on the analysis of yaw rate controllers by AFS. We developed several tests for benchmarking to minimize the effects of variables other than the independent variables which are special to each method. Consistent evaluation and comparative study by benchmarking are meaningful from the viewpoints not only that they lead us to promotion of our understanding but also that they show the limitations of each method which lead to the future research directions.

II. Vehicle Simulation Model

A. Model Validation by Experiment

A vehicle dynamics model with 10 DoF which consists of sprung rigid body (longitudinal/lateral motion, yaw, pitch, roll), front steering, and four independent wheels is developed in MATLAB/Simulink. This model has long been used in many former research of the authors' group. The slip ratio,

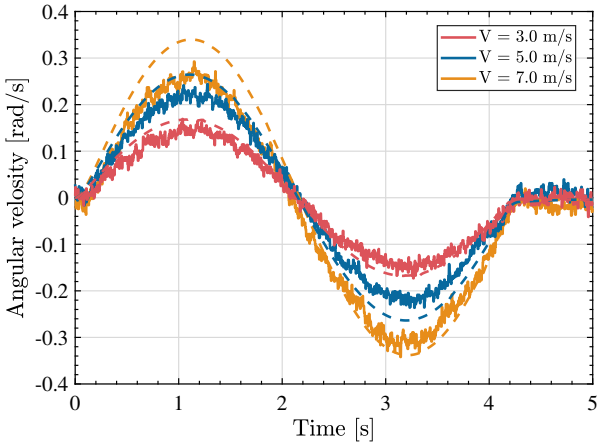

Fig. 1. Comparison of yaw rate between simulation (dashed line) and experiment (solid line).

TABLE I
VARIABLES OF THE VEHICLE MODEL.

front, rear	$i = \{\mathrm{f}, \mathrm{r}\}$
Vehicle velocity	V
Vehicle yaw rate	γ
Lateral acceelration	a_y
Vehicle sideslip angle	β
Wheel sideslip angle	α_i
Steering angle	δ

driving force, and lateral force are calculated by lambda-method [9] using the nonlinear tire slip model: Magic Fomula. It is assumed that lateral acceleration and yaw rate are measured by sensors which are usually installed in commercial cars. The main vehicle variables are summarized in Table I. An experimental vehicle held by the authors is assumed and its main parameters are summarized in Table II. The simulation model was validated by an test using the experimental vehicle aforementioned above. A sinusoidal steering angle reference was given while running at certain velocities. Yaw rates were measured by a digital gyro sensor via dSPACE Autobox and compared with simulation results in Fig. 1.

B. Nominal Model for Controllers

As the nominal model for the controllers, linear bicycle model (1)-(6) with 1 input and 1 outputs is extracted from the aforementioned nonlinear model. The vehicle velocity is assumed to be constant, and the steering angle is assumed to be small enough for first order approximation of Talor series.

$$\dot{x} = Ax + Bu, \tag{1}$$
$$y = Cx \tag{2}$$

TABLE II
PARAMETERS OF THE VEHICLE MODEL.

Vehicle mass m	880 kg
Vehicle yaw inertia I	617.0 kg $\cdot$ m^2
Distance between CoM and front axle l_f	0.999 m
Distance between CoM and rear axle l_r	0.701 m
Front cornering stiffness C_f	12500 N/rad
Rear cornering stiffness C_r	29200 N/rad

where

$$x = \begin{bmatrix} \beta \\ \gamma \end{bmatrix}, \ y = \gamma, \ u = \delta \tag{3}$$
$$A = \begin{bmatrix} -\dfrac{2}{mV}(C_\mathrm{f} + C_\mathrm{r}) & -1 - \dfrac{2}{mV^2}(l_\mathrm{f}C_\mathrm{f} - l_\mathrm{r}C_\mathrm{r}) \\ -\dfrac{2}{I}(l_\mathrm{f}C_\mathrm{f} - l_\mathrm{r}C_\mathrm{r}) & -\dfrac{2}{VI}(l_\mathrm{f}^2C_\mathrm{f} + l_\mathrm{r}^2C_\mathrm{r}) \end{bmatrix} \tag{4}$$
$$B = \begin{bmatrix} \dfrac{2C_\mathrm{f}}{mV} & \dfrac{2l_\mathrm{f}C_\mathrm{f}}{I} \end{bmatrix}^\top \tag{5}$$
$$C = \begin{bmatrix} 0 & 1 \end{bmatrix} \tag{6}$$

III. CONTROLLER DESCRIPTION

Among the AFS controllers proposed recently, we have selected the most promising ones: model predictive control (MPC), linear quadratic integral control (LQI) and yaw moment observer-based control (YMO).

A. Model Predictive Control

MPC is an optimal control method considering future state variables based on the nominal model (8) and current state variables to determine the input value. The cost function (7) consisting of the reference traceability of next prediction horizon N_p is minimized under constraints on input (9) and (10).

$$J = \sum_{k=1}^{N_\mathrm{p}} (\gamma_\mathrm{ref} - \gamma_k)^2 \tag{7}$$
$$x_{k+1} = A_\mathrm{d}x_k + B_\mathrm{d}u_k \tag{8}$$
$$u_\mathrm{min} < u_k < u_\mathrm{max} \tag{9}$$
$$\Delta u_\mathrm{min} < u_{k+1} - u_k < \Delta u_\mathrm{max} \tag{10}$$

The model (8) is the discrete model of (1) with sampling time T_s by zero-order hold. The cost functions used in MPC usually consists of a reference traceability term and an input size term. In this paper the input term is omitted since its maximum size is guaranteed by the constraint (9).

Optimization with feedback of state variables at each sampling time makes the system robust against uncertainties such as disturbances and modeling errors. On the other hand, MPC has a defect of calculation load.

Optimal inputs u_k $(k = 1 \sim N_\mathrm{p})$ are derived by solving the optimization problem, then u_1 is applied to the plant. There is a tradeoff between the controller performance and calculation time which is dependent on the lengths of T_s and N_p.

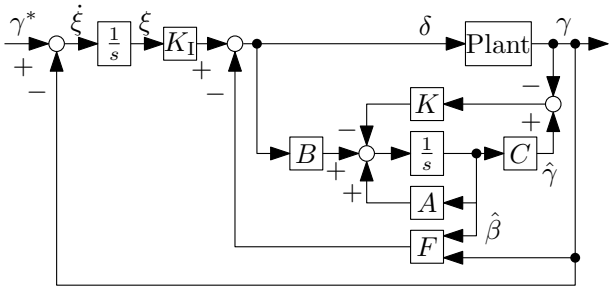

Fig. 2. Control structure of LQI.

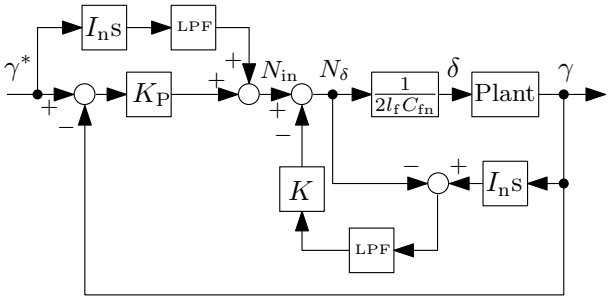

Fig. 3. Control structure of YMO.

B. Linear Quadratic Integral Control

The error dynamics model based on the linear bicycle model is

$$\begin{bmatrix}\dot{x}_e\\ \dot{\xi}_e\end{bmatrix} = \begin{bmatrix}A & 0\\ -C & 0\end{bmatrix}\begin{bmatrix}x_e\\ \xi_e\end{bmatrix} + \begin{bmatrix}B\\ 0\end{bmatrix} u_e(t) \tag{11}$$

where

$$x_e = x(t) - x(\infty),\ u_e = u(t) - u(\infty),\ \xi_e = \xi(t) - \xi(\infty) \tag{12}$$

and

$$u_e(t) = -\begin{bmatrix}F & K_\mathrm{I}\end{bmatrix}\begin{bmatrix}x_e\\ \xi_e\end{bmatrix}. \tag{13}$$

This system is able to be regarded as a regulator with state feedback. F is the state feedback gain vector and K_I is the integral gain in Fig. 2. From (11) and (13), closed loop error dynamics are given as

$$\begin{bmatrix}\dot{x}_e\\ \dot{\xi}_e\end{bmatrix} = \left(\begin{bmatrix}A & 0\\ -C & 0\end{bmatrix} - \begin{bmatrix}B\\ 0\end{bmatrix}\begin{bmatrix}F & K_\mathrm{I}\end{bmatrix}\right)\begin{bmatrix}x_e\\ \xi_e\end{bmatrix}. \tag{14}$$

The optimal u_e in (13) can be achieved with

$$\begin{bmatrix}F & K_\mathrm{I}\end{bmatrix} = R^{-1}B^TP \tag{15}$$

minimizing the objective function

$$J = \int_0^\infty \left\{x_e^\top(t)Qx_e(t) + u_e^\top(t)Ru_e(t)\right\}\mathrm{d}t. \tag{16}$$

P in (15) is the solution of Riccati equation to stabilize the error dynamics system (14) corresponding to (16).

Since sideslip angle, one of the state variables to feedback, can not be measured directly, Luenberger observer was used to estimate the variable as in Fig. 2.

C. Yaw Moment Observer-Based Control

A yaw rate control method using YMO and lateral force observer (LFO) for electric vehicles with in-wheel motors was proposed in [10]. This method utilizes the difference of driving forces between left and right in-wheel motors to generate direct yaw moment while estimating and compensating other yaw moments to nominalize the plant. AFS is also used to control lateral motion by nominalizing the plant with a LFO in [10].

A YMO-based yaw rate control method by AFS was proposed in [11] in a similar way to [10] without using in-wheel motors. The yaw motion equation, the second row of (1) can be described using N_δ and $N_{\beta\gamma}$ as follows:

$$\begin{aligned} I\dot{\gamma} &= 2l_\mathrm{f}C_\mathrm{f}\delta + \left(-2\left(l_\mathrm{f}C_\mathrm{f} - l_\mathrm{r}C_\mathrm{r}\right)\beta - \frac{2}{V}\left(l_\mathrm{f}^2C_\mathrm{f} + l_\mathrm{r}^2C_\mathrm{r}\right)\gamma\right)\\ &= N_\delta + N_{\beta\gamma} \end{aligned} \tag{17}$$

$N_{\beta\gamma}$ is estimated by the observer in Fig. 3. By compensating $N_{\beta\gamma}$, the plat can be nominalized as

$$\gamma = \frac{1}{I_\mathrm{n}\mathrm{s}}N_\mathrm{in} \tag{18}$$

under the cut-off frequency of the low-pass filter.

Feedforward and proportional feedback control are applied to the nominalized plant by pole assignment.

IV. Evaluation Description

For the sake of relative comparison, the index values are normalized relatively to the maximum index values among the controllers.

A. Slew Rate of Actuator Input Value

Steering angle inputs to the actuator EPS generated by each controller are evaluated relatively when the output yaw rates by each method are following a reference enough.

Since drastical changes in a steering angle input are not preferable, the maximum value of the inverse of the slew rates of the steering angle input values generated by the controllers

$$\max\left\{\|\mathrm{d}\delta/\mathrm{d}t\|^{-1}\right\} \tag{19}$$

is defined as the performance index of each controller.

A sine and dwell wave form with the frequency 0.7 Hz and the amplitude 0.1 rad/s is used as the yaw rate reference.

B. Reference Tracking Performance in Emergency Situations

This performance index evaluates the tracking performance to a drastically changing yaw rate reference which leads to input saturation. This is typically seen in emergency collision avoidance situations.

A sine and dwell wave form with frequency 0.7 Hz and amplitude 0.75 rad/s is used as the yaw rate reference. This wave form consisting of a drastical steering and reverse

steering simulates a typical driver's handling who is in panic in front of an obstacle.

Since integrals of yaw rate errors are important, the inverse of the root mean square (RMS) of tracking errors

$$\left(\sqrt{\sum_{k=1}^{N}\left(\gamma\left[k\right]-\gamma^{\mathrm{ref}}\left[k\right]\right)^{2}}\right)^{-1} \tag{20}$$

is defined as the performance index of the controllers. N is defined by (simulation time)/(sampling time).

C. Robustness Performance against Yaw Moment Disturbances

The robustness against yaw moment disturbances is evaluated in this performance index. The yaw moment disturbances are assumed to be caused by split-μ braking; e.g. brakes on snowy or wet roads of which slip ratios on left and right sides are different.

The given yaw rate reference is fixed to 0 and step disturbance of 2000 Nm was applied around the center of the gravity of the vehicle.

The 5% settling time was evaluated as the robustness performance index.

D. Stability Performance of Sideslip Angle

Besides yaw rate, another important state variable to represent vehicle dynamics is sideslip angle β [12]. This variable represents the deviation of the direction of vehicle velocity from the direction of the body. The smaller the sideslip angle is, the more stable the vehicle is.

A sine wave with frequency 0.33 Hz and amplitude 0.15 rad/s is used as the yaw rate reference. This reference is for the situation of a vehicle running at 60 kph to change lanes by moving about 3.5 m to lateral direction in 3.0 s.

The inverse of RMS of sideslip angle

$$\left(\sqrt{\sum_{k=1}^{N}\beta\left[k\right]}\right)^{-1} \tag{21}$$

was evaluated as the stability performance index.

V. Simulation Results

Parameters

The parameters of MPC were set as follows: sampling time $T_{\mathrm{s}} = 10$ ms, prediction horizon $N_{\mathrm{p}} = 10$ and uppler and lower limits of the constraints (9) and (10) $u_{\max} = -u_{\min} = 0.35$ rad, $\Delta u_{\max} = -\Delta u_{\min} = 0.175$ rad/s. Although disturbance rejection performance improves as the sampling time T_{s} becomes small, the computational effort increases as T_{s} deceases. On the other hand, although the length of the predictive horizon N_{p} is the number of future control intervals and plays an important role of optimization results, the controller memory requirements and QP solution time increases as N_{p} increases. In this paper, T_{s} was determined to make the evaluation value of section IV-A close to other two methods. N_{p} was determined as a small number while preserving the performance. The constraint parameters were determined according to the expermental setup's requirements.

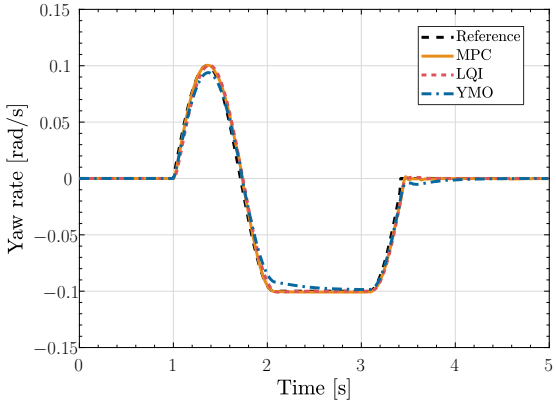

Fig. 4. Slew rate test (yaw rate).

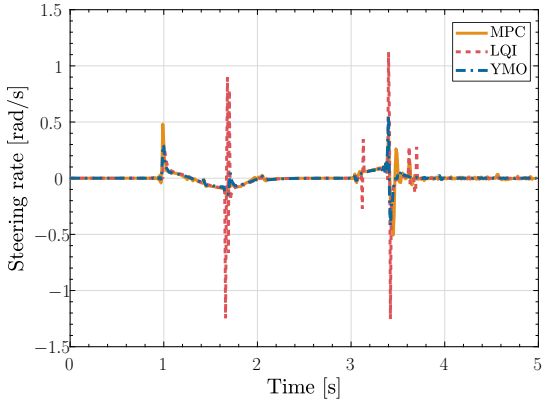

Fig. 5. Slew rate test (slew rate of steering angle).

With respect to LQI, the pole of the observer was set to 20 rad/s to sufficiently estimate β. The weights in the objective function (16) were $Q \gg R$ which minimize only the yaw rate error as well as the cost function of MPC.

As for YMO controller, the cut-off frequency of low-pass filter was $\omega_{\mathrm{LPF}} = 30$ rad/s to sufficiently nominalize the plant. The compensation gain K in Fig. 3 was $K = 1$. The outer loop pole was 5 rad/s which is about one order slower than the inner loop cut-off frequency.

As is the case of MPC, steering actuator limit of ± 0.35 rad was applied to the other two controllers.

A. Slew Rate of Actuator Input Value

Fig. 4 shows that there is almost no difference among the yaw rate outputs. It is, however, recognized in Fig. 5 that the slew rates of actuator input to realize the same outputs are different. The index values defined in section IV-A are; MPC: 1.0, LQI: 0.40, YMO: 0.91.

B. Reference Tracking Performance in Emergency Situations

Fig. 6 and Fig. 7 show that the yaw rate and the steering angle differ in the emergency situation. The remarkable differ-

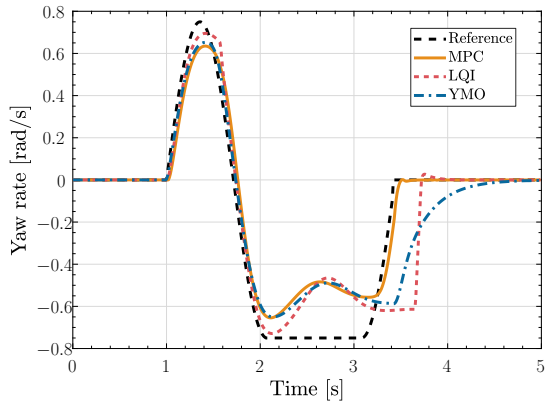

Fig. 6. Traceability in emergency situation test (yaw rate).

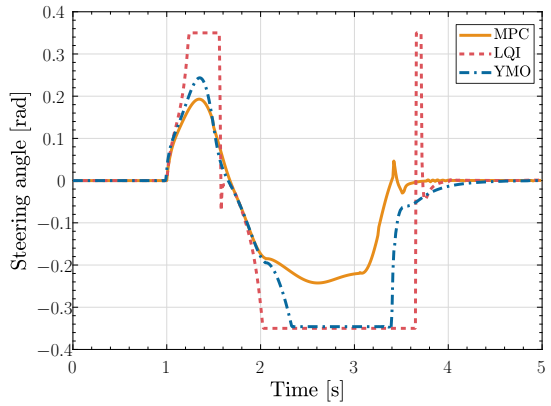

Fig. 7. Traceability in emergency situation test (steering angle).

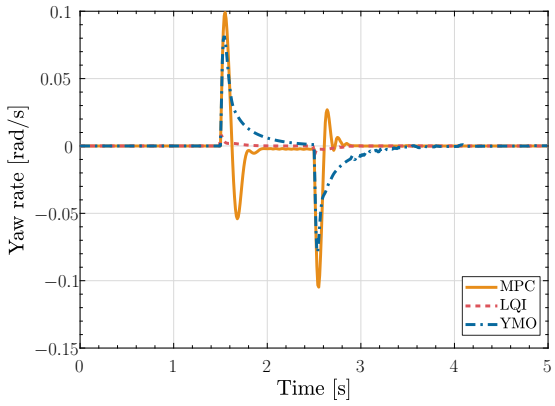

Fig. 8. Robustness against yaw moment disturbance test (yaw rate).

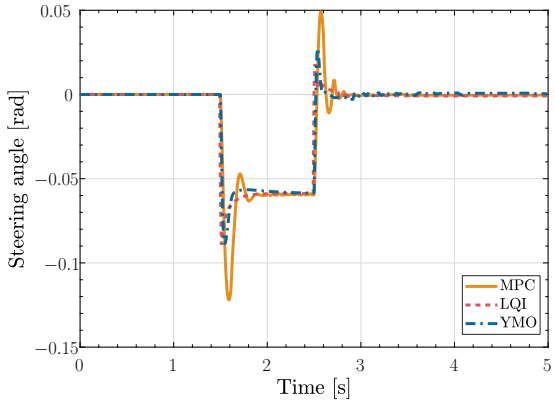

Fig. 9. Robustness against yaw moment disturbance test (steering angle).

ence is that LQI and YMO methods were led to actuator input saturation while MPC was not. This phoenomenon explains the differences of the index performance; MPC: 1.0, LQI: 0.41, YMO: 0.069. The big differences in the result was led by the advantage of MPC that the actuator limits are conserved during the optimization of actuator inputs.

C. Robustness Performance against Yaw Moment Disturbances

Fig. 8 and Fig. 9 show the yaw rates and steering angle with yaw moment disturbance. The settling speeds and the states of overshoot are different among the methods. The index values defined in section IV-C are represented as follows; MPC: 0.90, LQI: 1.0, YMO: 0.56.

D. Stability Performance of Sideslip Angle

The yaw rates and the sideslip angles are shown in Fig. 10 and Fig. 11. It can be seen that there is little difference in RMS of sideslip angle among the methods. The index values are: MPC: 0.90, LQI: 0.91, YMO: 1.0.

VI. Conclusion

The proposed study focused on the cross comparison among the state-of-the-art yaw rate control methods by AFS. Four performance indices were defined: the slew rate of actuator input, the reference tarcking performance in emergency situation, the robustness performance against yaw moment disturbance, and the sideslip angle stability.

The comparison was carried out in a simulation environment with a 10 DoF vehicle dynamics model validated by an experiment among the controllers: MPC, LQI, and YMO-based controller. The relative evaluation results of the three controllers in terms of the four performance indices are shown in Fig. 12.

Acknowledgment

This work has received funding from the European union Horizon 2020 research and innovation program H2020-MSCA-RISE-2016 under the grant agreement No. 734832 CLOVER project. This work was partly supported by JSPS KAKENHI Grant Number 18H03768, Industrial Technology Research Grant Program from New Energy and Industrial Technology Development Organization (NEDO) of Japan (number 05A48701d) and the Ministry of Education, Culture, Sports, Science and Technology grant (number 22246057 and 26249061).

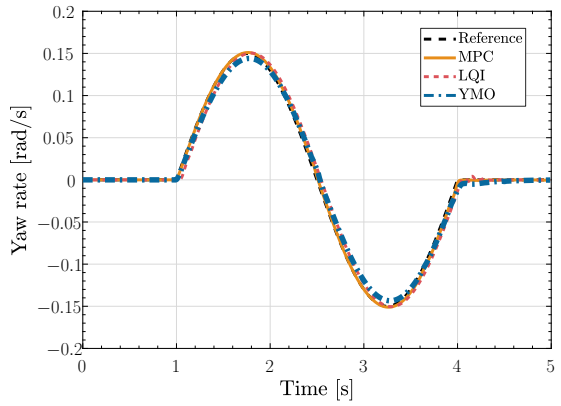

Fig. 10. Sideslip angle stability test (yaw rate).

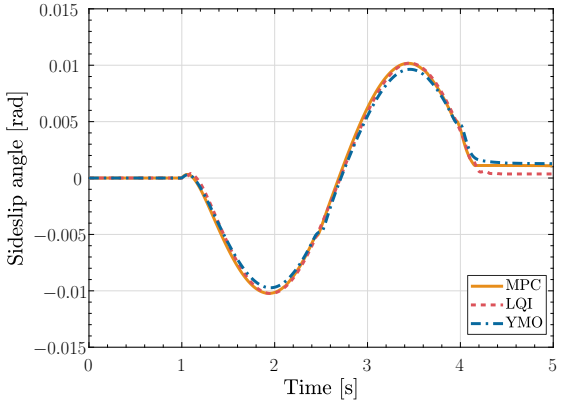

Fig. 11. Sideslip angle stability test (sideslip angle).

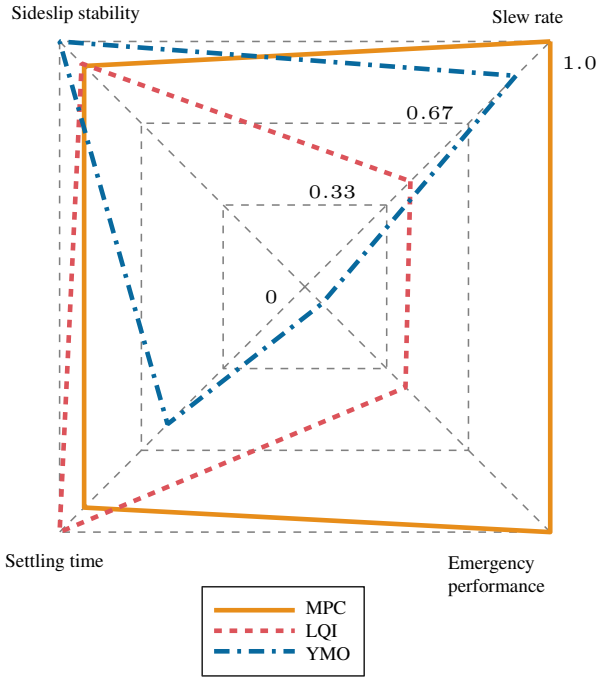

Fig. 12. Relative evaluation by performance indices.

REFERENCES

[1] ABC News, "New video shows moments before fatal self-driving Uber crash," https://www.youtube.com/watch?v=ufNNuafuU7M, [Jun. 7, 2019].

[2] Baptiste Rouzier, Mehdi Hazaz, Toshiyuki Murakami, and Weiliang Xu. "Application of Active Driving Assist to Remotely Controlled Car in Collision Avoidance" IEEJ J. Industry Applications, vol. 7, no. 4, pp. 289-297, 2018.

[3] Zainab Zainal, Wan Rahiman, and M. N. R. Baharom. "Yaw Rate and Sideslip Control Using PID Controller for Double Lane Changing." Journal of Telecommunication, Electronic and Computer Engineering (JTEC) vol. 9 no. 3-7, pp. 99103, 2017.

[4] E. Kim, J. Kim, and M. Sunwoo. "Model Predictive Control Strategy for Smooth Path Tracking of Autonomous Vehicles with Steering Actuator Dynamics" International Journal of Automotive Technology and Management vol. 15, no. 7, pp. 115564, 2014.

[5] Nematollah Tavan, Mehdi Tavan, and Rana Hosseini. "An Optimal Integrated Longitudinal and Lateral Dynamic Controller Development for Vehicle Path Tracking" Latin American Journal of Solids and Structures vol. 12, no. 6, pp. 100623, 2015.

[6] Xinbo Ma, Pak Kin Wong, Jing Zhao, and Zhengchao Xie. "Multi-Objective Sliding Mode Control on Vehicle Cornering Stability with Variable Gear Ratio Actuator-Based Active Front Steering Systems" Sensors vol. 17, no. 1, 2016.

[7] Kanghyun Nam, Sehoon Oh, Hiroshi Fujimoto, and Yoichi Hori. "Robust Yaw Stability Control for Electric Vehicles Based on Active Front Steering Control through a Steer-by-Wire System" International Journal of Automotive Technology and Management, vol. 13, no. 7, pp. 116976, 2012.

[8] Valentin Ivanov, Dzmitry Savitski, Klaus Augsburg, Schalk Els, Cor-Jacques Kat, Theunis Botha, Miguel Dhaens, Corina Sandu, Rui He, Sterling McBride, Angel Gabriel Alatorre Vazquez, and Alessandro Correa Victorino. "Challenges of Integrated Vehicle Chassis Control: Some Findings of the European Project EVE" IEEJ J. Industry Applications, vol. 8, no. 2, pp. 218-230, 2019.

[9] Y. Horiuchi. "A proposition of the simple tire model for the Vehicle Stability Assist system." Society of Automotive Engineers of Japan, preceding of congress, No.64-98, 1998. (in Japanese)

[10] Hiroshi Fujimoto, and Yuya Yamauchi. "Advanced Motion Control of Electric Vehicle Based on Lateral Force Observer with Active Steering." In 2010 IEEE International Symposium on Industrial Electronics, pp. 362732, 2010.

[11] Hiroaki Kitano, Osamu Nishihara, Masahiko Kurishige, and Takanori Matsunaga. "Estimation of Lateral Disturbance with Observer and Compensation Control with Electric Power Steering" Transactions of the Japan society of mechanical engineers. C, vol. 78, no. 795, pp. 3715–3729, 2012. (in Japanese)

[12] Bangji Zhang, Haiping Du, James Lam, Nong Zhang, and Weihua Li. "A Novel Observer Design for Simultaneous Estimation of Vehicle Steering Angle and Sideslip Angle." IEEE Transactions on Industrial Electronics, vol. 63, no. 7, pp. 435766, 2016.